Commercial Satellite Data Acquisition Program

GHGSat Atmospheric Column Quality Assessment Report

Goddard Space Flight Center
Greenbelt, MD

Commercial Satellite Data Acquisition Program GHGSat Atmospheric Column Quality Assessment Report

Signature/Approval Page

Approval by:

Melissa Yang Martin Commercial Satellite Data Acquisition Program Manager Earth Science Division Headquarters/NASA	Date

Accepted by:

Dana Ostrenga Commercial Satellite Data Acquisition Project Manager Earth Science Division GSFC/NASA	Date

Preface

This document is under CSDA Project configuration control. Once this document is approved, CSDA approved changes are handled in accordance with Class I and Class II change control requirements described in the CSDA Configuration Management Procedures based on NASA standard configuration practices, and changes to this document shall be made by document change notice (DCN), documented in the Change History Log or by complete revision.

Abstract

The evaluation summarized in this report was conducted by subject matter experts (SMEs) funded by NASA's Commercial Satellite Data Acquisition (CSDA) Program. The SMEs evaluated the radiometric and geometric quality of GHGSat data for the NASA Earth science research and applications community. The results of the evaluation help to inform NASA program management on the quality of the data for NASA science.

Cover Art: Cover art is AI generated graphic using Microsoft Copilot Designer using term "commercial satellite constellation Earth observation across Atlantic AND Northern Hemisphere AND digital downlink"

Authored and prepared by

John Worden
GHGSat Evaluation Team Lead and
Atmospheric Composition Subject Matter Expert
Jet Propulsion Laboratory
National Aeronautics and Space Administration

Clayton Elder
GHGSat Evaluation Team Member
Jet Propulsion Laboratory
National Aeronautics and Space Administration

Ben Poulter
GHGSat Evaluation Team Member
National Aeronautics and Space Administration

Nikolay Balashov
GHGSat Evaluation Team Member
National Aeronautics and Space Administration

Max Krause
GHGSat Evaluation Team Member
Environmental Protection Agency

Danielle Wood
GHGSat Evaluation Team Member
Massachusetts Institute of Technology (MIT)

Davida Street
GHGSat Evaluation Team Member
National Oceanic and Atmospheric Administration

Frederick Policelli
CSDA Project Scientist
National Aeronautics and Space Administration

Jaime Nickeson
CSDA Technical Science Coordinator
Science Systems and Applications, Inc.
National Aeronautics and Space Administration

Change History Log

Revision	Effective Date	Description of Changes
1.0	03/22/2024	First Draft Completed
1.0	11/20/2024	Reviewed and reformatted into CSDA outline

Table of Contents

List of Figures

List of Tables

Acronyms & Abbreviations

ATBD	Algorithm Theoretical Basis Document
AVIRIS-NG	Airborne Visible-Infrared Imaging Spectrometer - Next Generation
CF	Climate & Forecast (Metadata Convention)
CEOS	Committee on Earth Observation Satellites
CSDA	Commercial Satellite Data Acquisition
DN	Digital Number
DOI	Digital Object Identifier
EDAP	Earthnet Data Assessment Pilot
EMIT	Earth Surface Mineral Dust Source Investigation
EO	Earth Observation
ESA	European Space Agency
EULA	End-User License Agreement
FAIR	Findable, Accessible, Interoperable and Reusable
FRM	Fiducial Reference Measurement
FWHM	Full Width Half Maximum
GUM	Guide to the Expression of Uncertainty in Measurement
INSPIRE	Infrastructure for Spatial Information in Europe
L1	Level 1
L2	Level 2
LSF	Line Spread Function
MTF	Modulation Transfer Function
MSI	Multispectral Instrument (on Sentinel-2 platform)
NASA	National Aeronautics and Space Administration
NOAA	National Oceanic and Atmospheric Administration
NPL	National Physical Laboratory, UK
OLI	Operational Land Imager (instrument on Landsat 8)
PCC	Pearson Correlation Coefficient
PSF	Point Spread Function
PUG	Product User Guide
PUM	Product User Manual
QA	Quality Assessment
QA4EO	Quality Assurance Framework for Earth Observation
QA4ECV	Quality Assurance Framework for Essential Climate Variables
RMSE	Root Mean Squared Error
S2	Sentinel-2
SI	Système International (International System of Units)
SSR	Sensor Spatial Response
TROPOMI	Tropospheric Monitoring Instrument
URL	Universal Resource Locator
VZA	View Zenith Angle

Executive Summary

The CSDA Program was established to identify, evaluate, and acquire data from commercial sources that support NASA's Earth science research and application goals. NASA's Earth Science Division (ESD) recognizes the potential impact commercial satellite constellations may have in encouraging/enabling efficient approaches to advancing Earth System Science and applications development for societal benefit. Commercially acquired data may also provide a cost-effective means to augment and/or complement the suite of Earth observations acquired by NASA and other U.S. government agencies and those by international partners and agencies.

This quality of the GHGSat emission product was evaluated using input from the CSDA evaluation team, following a recently developed draft of the Joint NASA/ESA assessment guideline for greenhouse gas (GHG) emission data. The evaluation lead was enlisted to assess the fundamental quality of the GHGSat data using only results from the CSDA evaluation and documented descriptions of the GHGSat concentrations and emissions from GHGSat. Details about the utility of GHGSat data for NASA science is available in a separate CSDA Program Evaluation Report. This quality assessment reflects only the current understanding of the GHGSat constellation and reported measurements. Additional relevant input as well as changes to the technology could necessitate updates to this assessment.

At the time of the evaluation, GHGSat had a constellation of 10 satellites equipped with Fabrey-Perot hyperspectral imaging spectrometers, that have a field of view of 12 x 12 km, collecting 30 m resolution data with a nominal revisit period of approximately 14 days. GHGSat produces a Level-2 (L2) abundance dataset in GeoTIFF format, a Level-2 concentration map in PNG format, and a Level-4 (L4) emissions product as text (PDF, CSV). The abundance dataset includes per-pixel abundances of column average mixing ratio or column density, along with associated measurement errors. This document is an evaluation of the L4 methane emission estimation only. The assessment presented in this document is divided into two main parts: a documentation review and an assessment of the data. The documentation review in sections 2.1 through 2.3 includes the assessment of the information contained in the documents provided to the CSDA evaluation team by GHGSat. The grading of the information provided is given in the left portion of the Summary Product Evaluation Matrix shown in Figure 1. Sections 3 and 4 summarize the evaluation performed by the NASA teams using the data purchased through the CSDA program. This evaluation is summarized in the last column of Figure 1. Sections 3 and 4 provide more detailed explanations on the methods and the results of the assessment used to arrive at the validation summary column and are shown in the more detailed Validation Maturity Matrix (see Figure 2).
The GHGSat Level-2 concentration enhancement map identifies the target methane plume, which is highlighted from the background image using a pseudocolor mapping to depict concentration levels. Plumes of methane are then identified by first quantifying pixels with enhanced concentration values relative to background and then an algorithm is applied to determines if a coherent plume structure can be identified from these enhanced values.

1 Cal/Val Maturity Matrices

1.1 Summary Cal/Val Maturity Matrix

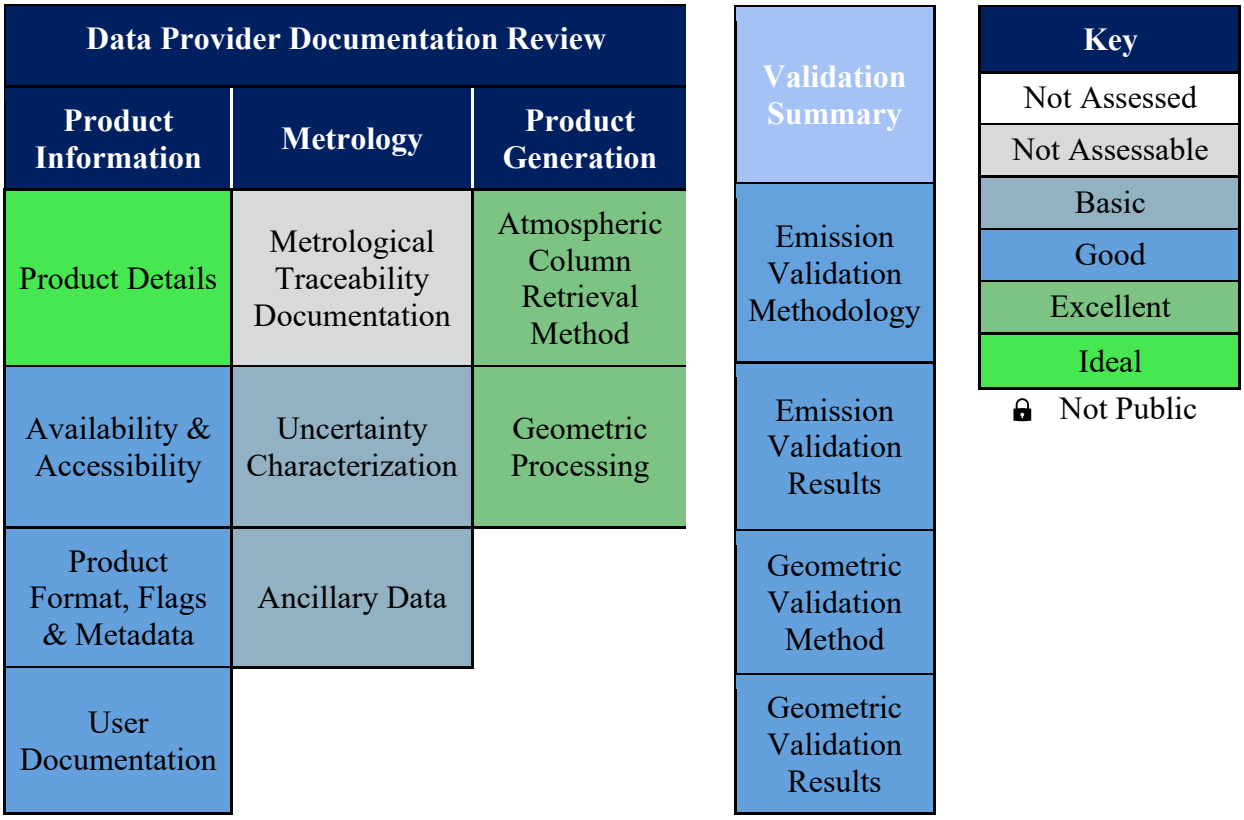

Figure 1. Summary Cal/Val Maturity Matrix

1.2 Detailed Validation Maturity Matrix

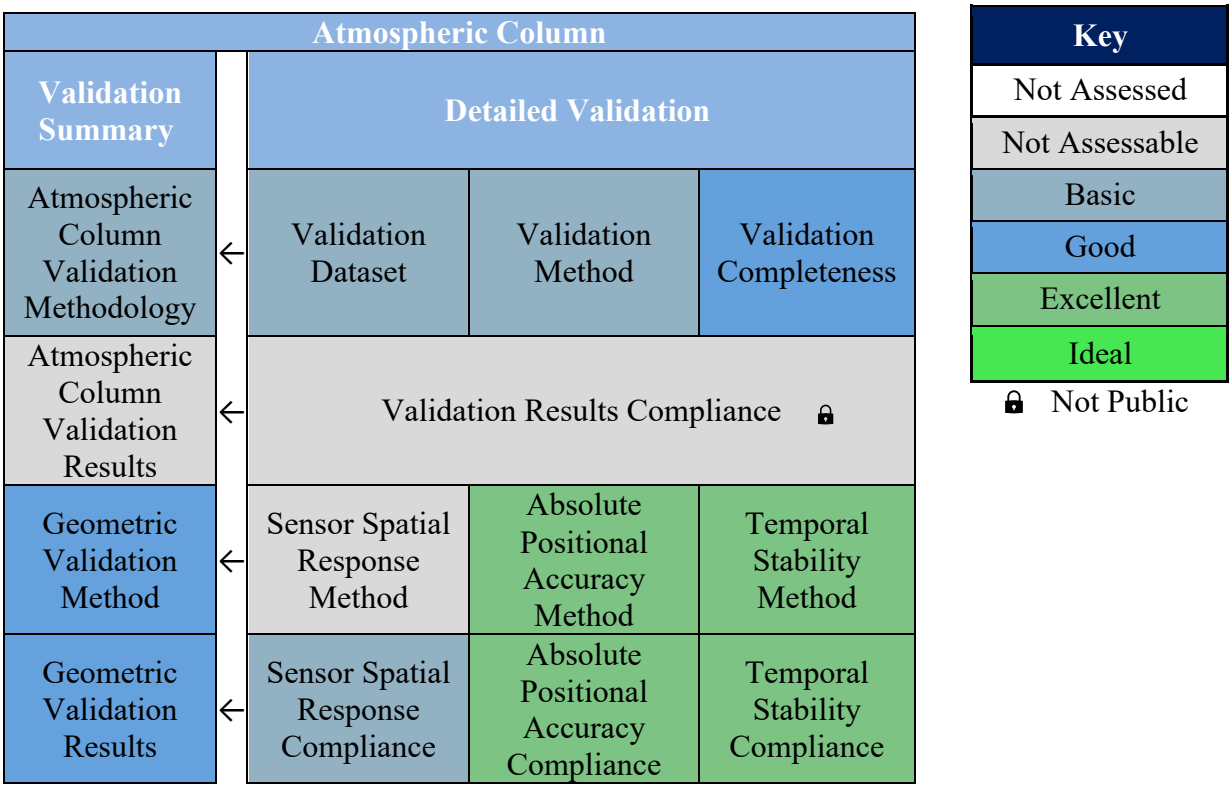

Figure 2. Detailed Validation Maturity Matrix, showing the Validation Summary column from the Summary Cal/Val Maturity Matrix.

2 Data Provider Documentation Review

2.1 Product Information

Product Details	
Grade: Ideal	
Justification	All required information was made available and was sufficient download and use the data.
Product Name	GHGSat emission rate
Sensor Name	GHGSat-C1, -C2, -C3, -C4, -C5, -C6, -C7, -C8, -C9, -C10
Sensor Type	Fabry-Perot Imaging Spectrometer

Mission Type	Hyperspectral SWIR Constellation
Mission Orbit	Sun Synchronous, low earth orbit, nearly global coverage (except 3.7deg cone at poles)
Product Version Number	Processing version 8.11.0
Product ID	CH4SM
Processing level of product	Level 4
Measurement Quantity Name	Emission rate
Measurement Quantity Units	Kg CH_4/hr
Measurement Quality	GHGSat claims a detection threshold of 100 kg (CH_4)/h at 3 m/s winds, with methane column density precision at 1% of background, and claims a non-specific sub-pixel (< 30 m) geolocation accuracy.
Spatial Coverage	~12 x 12 km
Point of Contact	Eric Choi (echoi@ghgsat.com)
Product locator (DOI/URL)	10.5194/amt-14-2127-2021; GHGSat document ID: GHG-1347-6001-c
Conditions for access and use	USG+ EULA, for research and scientific use only
Product Abstract	Emission rate from a targeted source estimated using abundance dataset(s) and applying dispersion modelling techniques.

Availability & Accessibility	
Grade: Good	
Justification	The data set meets some of the FAIR principles, they are easily findable, the metadata is well-organized, and defined, stored in JSON files. The data management plan is unknown currently, but the data package shows progress towards the FAIR principles. Metadata would not be described as rich. Bulk download was not a readily available option and had to be requested.
Compliant with FAIR principles	No
Data Management Plan	Unknown
Availability Status	Data are available from GHGSat's Spectra interface after purchasing license for use.

Product Format	
Grade: Good	
Justification	Data exist in a documented standard file format (GeoTIFF). No other file formats are offered. Includes a good set of documented metadata and data flags. Explanation and details on some of the quality flags are lacking. As discussed in the CSDA evaluation, the Metadata could be more complete
Product File Format	GeoTIFF
Metadata Conventions	Partial
Analysis Ready Data?	No

User Documentation		
Grade: Good		
Justification	GHGSat does not a have a document that is referred to as a user guide. Some product user guide type of information is available but is contained within multiple documents and some literature. Documentation is up to date. An algorithm theoretical basis document (ATBD) is available.	
Document	**Reference**	**QA4ECV Compliant**
Product User Guide	"Data_File_Description", "Technical_Orientation", and "CSDA+Comprehensive+Data+Catalogue" documents were used. The latter also contained a peer-reviewed publication within.	No
ATBD	**GHGSat Document ID: GHG-1639-4001-a** A document that GHGSat considers to be proprietary.	No

2.2 Metrology

Metrological Traceability Documentation	
Grade: Not Assessable	
Justification	Not assessable, no traceability chain documented.
References	GHGSat ATBD (note this proprietary information)

Uncertainty Characterization	
Grade: Basic+	
Justification	Uncertainties for the atmospheric column enhancements are provided and a description of how these uncertainties are calculated are described in the ATBD. However, a good rating could not be provided because a description of how albedo variation affects the methane plume mask is not provided.
References	Product files and the ATBD

Ancillary Data	
Grade: Good	
Justification	The ATBD indicates that ancillary data are used to estimate methane concentrations (e.g. Landsat Albedo, AIRS CH_4, CO_2, and H_2O) but these are not provided with the product files.
References	Product files and ATBD

2.3 Product Generation

Atmospheric Column Retrieval Algorithm	
Grade: Excellent	
Justification	The column retrieval algorithms are described in a publicly reviewed paper and also in the ATBD.
References	The GHGSat imaging spectrometer (https://amt.copernicus.org/articles/14/2127/2021/) article and the GHGSat ATBD.

Geometric Processing	
Grade: Excellent	
Justification	Standard procedures are followed and documented. Results of testing would be ideal to see. See section 4, Detailed Validation – Geometric.
References	GHGSat Inc. (2022), "GHGSat Constellation Imagery and Data NASA CSDA Comprehensive Data Catalogue" Document No. GHG-1347-6001.

Mission-Specific Processing	
Grade: Not Assessable.	
Cloud Mask	
Justification	Additional processing steps not documented.
Reference	
Quality Flags	
Justification	Additional processing steps not documented.
Reference	

3 Detailed Atmospheric Column Validation

3.1 Validation Methodology

3.1.1 Validation Dataset

As part of the NASA Commercial Satellite Data acquisition program, comparisons were made between GHGSat concentration and emission data with the same data from NASA's Earth Surface Mineral Dust Source Investigation (EMIT) instrument. In this section we use the EMIT / GHGSat comparisons as the basis for assessing the atmospheric column validation. Figure 3 demonstrates consistency between the EMIT and GHGSat plumes over a selected scene. However, this is not a formal validation as the GHGSat concentrations are not being compared to a well-calibrated, validated measurement; EMIT concentrations themselves have only been indirectly validated. The

GHGSat concentration plumes have also been compared to the Tropospheric Monitoring Instrument (TROPOMI) concentrations (Varon et al. 2019). While TROPOMI data have been validated through comparisons with ground-based Fourier transform spectrometer data, the differences in spatial resolution and sampling make it challenging to directly compare GHGSat with TROPOMI data. For these reasons we grade the validation data sets for the GHGSat atmospheric column data as “Basic”.

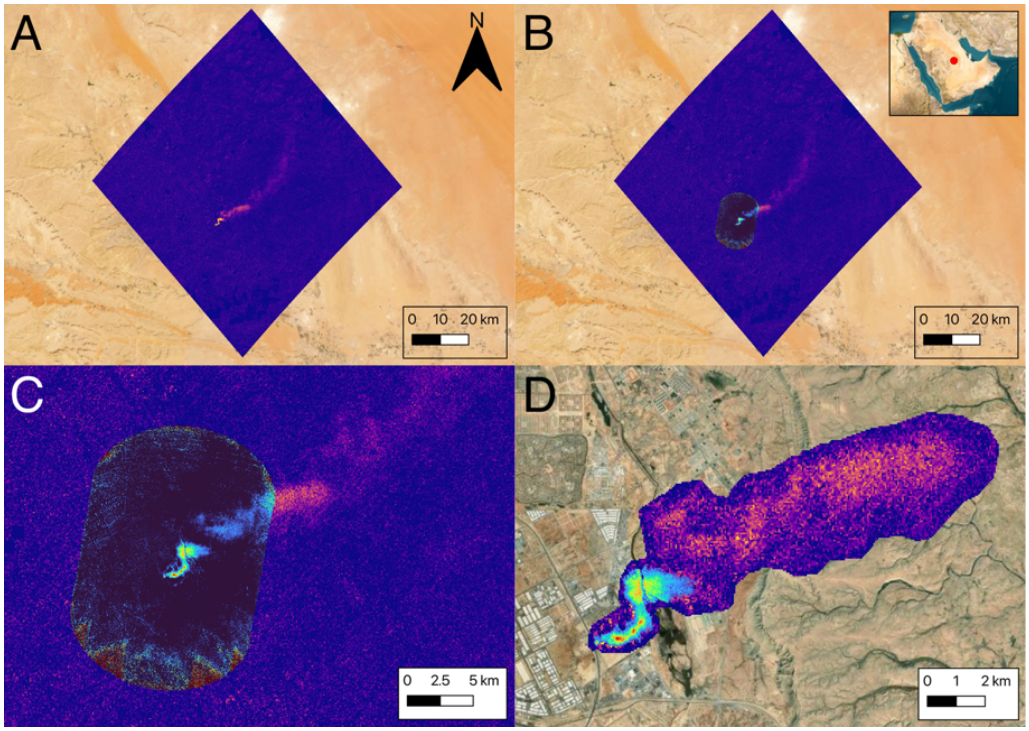

Figure 3. How the methane concentrations in GHGSat data (oval in panel C) overlap those from EMIT (square, Panel C).

3.1.2 Validation Method

The comparison of GHGSat data with EMIT and TROPOMI shows consistency in observed methane concentrations associated with plumes (i.e. all 3 data sets generally show enhanced concentrations with a similar profile shape). However, this comparison approach only indirectly validates the GHGSat data. For this reason, and because the criteria for the grade of “Good” requires a mature validation approach, the validation method grade given here is “Basic”.

3.1.3 Validation Completeness

Comparisons are made for a variety of different scenes, over one season; we therefore grade the validation completeness as “Good”.

3.2 Validation Results

3.2.1 Validation Results Compliance

As we do not have documentation on the “claimed mission performance” the validation results compliance is indicated as ‘Not assessable’.

4 Detailed Validation - Geometric

4.1 Sensor Spatial Response

4.1.1 Method

The sensor spatial response testing and methods in the GHGSat documentation provided were not described in enough detail for us to assess the quality of their SSR process, which is why it was marked as ‘Not Assessable’ in the matrix (Figure 2).

We assessed the sensor spatial response with images over two California bridges, the Golden Gate (23 m wide) and the eastern portion of the San Mateo (41 m wide). A line spread analysis can be performed here where there is a regular, long, bright bridge against an ideally constant black water background. The bridges are slightly slanted from the image grid direction. Four GHGSat images were allocated to the geolocation quality assessment and acquisitions over these bridges were requested. One acquisition was delivered over the San Mateo Bridge while the other three were acquired over the Golden Gate Bridge. One sensor, GHGSat C5, imaged both bridges. The C2 and C7 sensors acquired the other Golden Gate Bridge images. The GHGSat ALB image product (albedo, surface reflectance) was used in this analysis.

For each along row or along column direction, the assessment uses at least 20 x 20 rows and columns, with the bridge at the center (see Figure 4a). A bridge center line location was estimated based on visual inspection of each image. Pixels are then transformed from bins to distance (Figure 5) from the center line with the equation

$$dp = d*\cos(\Theta), \quad (1)$$

where Θ is the angle between the line and vertical/horizontal, d is the vertical/horizontal distance from the pixel center to the transition line, and dp is the perpendicular distance from pixel center to the transition line.

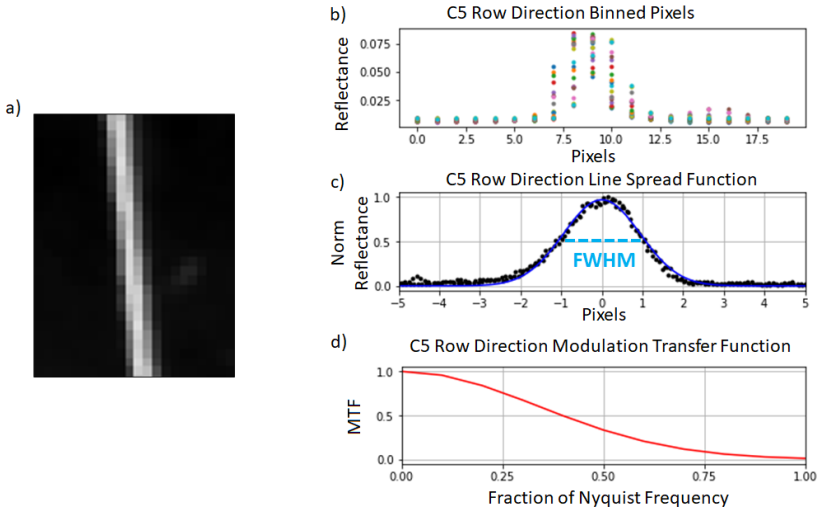

Figure 4. Visual demonstration of SSR calculations. a) GHGSat (C5) over the Golden Gate Bridge site used in the SSR calculations. b) Binned pixels read in from Fig.4a, colored by row. c) Sub-pixel impulse response constructed based on Fig.5 (black points) with a gaussian fit line (blue) for the Line Spread Function (LSF). FWHM is shown in blue dashed lines, here it is 2.0 pixels. d) Modulation Transfer Function (MTF) is the Fourier Transform of the LSF (Fig.4c). Here, the x axis is normalized by Nyquist Frequency = 1 cycle in 2 pixels and y-axis is MTF value that may be regarded as contrast retention for the two pixels apart at the corresponding spatial frequency.

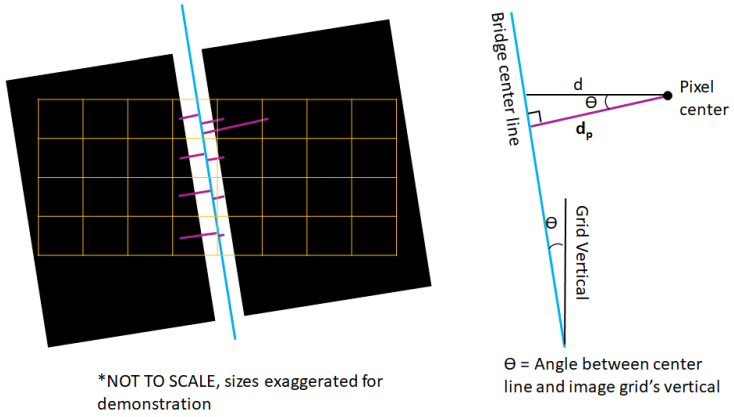

Figure 5. Schematic concept of the transformation from pixel bins to distance from bridge centerline over a background. The bridge center line is marked by the blue line, the yellow grid represents the image pixel grid, and the purple lines represent the distance from pixel center to bridge center line. The schematic to the right is a simplified version of the graphic on the left. This allows calculation of the sub-pixel transition from black to white to black for the LSF

Once the values are transformed into distance from the center line, a gaussian function is fit to the line, creating a Line Spread Function (LSF) (Fig. 4c). Full Width at Half Maximum (FWHM) is found from this LSF that represents the sensor's effective footprint size. Finally, the Fourier transform of the LSF gives the Modulation Transfer Function (MTF) (Fig. 4d). One more metric for spatial response is found with the MTF curve, the MTF value at Nyquist frequency. We will evaluate GHGSat's spatial response with FWHM as its effective footprint size.

The bridge width can change the apparent FWHM analyzed in the images using the above method. To account for this, we have run simple models to simulate how the true bridge width imaged by

LSFs of various FWHMs changes apparent FWHM in the resulting image. The results of the modelling are below, the relationship changes if the bridge width is less than or more than the LSF FWHM. When the width is far less than the FWHM, the apparent FWHM is equal to the LSF FWHM. This is the case for the Golden Gate Bridge (Fig. 6a). When the bridge is compatible with or wider than the LSF FWHM, the apparent FWHM is widened, which is the case for the San Mateo Bridge. The modelled relationship in Figure 6b allows us to account for bridge width in our analysis.

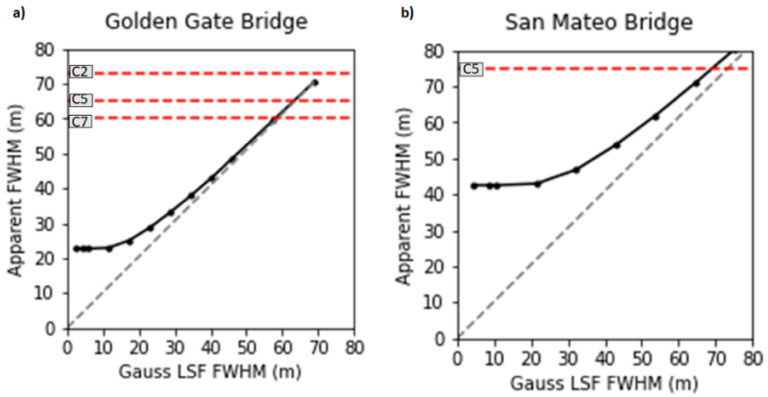

Figure 6. Modelling results of bridge width and true LSF impacts on measured apparent PSF FWHM. Results are applied to a) the Golden Gate Bridge and b) the San Mateo Bridge. Black line shows the modelled relationship between Gaussian PSF FWHM and measured apparent FWHM, Gray dashed line marks the 1:1 ratio, and red dashed horizontal lines mark the measured apparent FWHM in our results. The "Gauss LSF FWHM" values at the intersections of the modelled curves and the horizontal lines are true approximation of the sensor spatial resolution.

Our process follows the standard method of spatial response assessment, but it does not account for some sources of error such as bridge non-uniformity (structures, cars, etc.) and atmospheric interference. These factors tend to make the assessed FWHM larger. We have evaluated 3 out of 10 sensors, one of which is evaluated in both row and column directions.

4.1.2 Results Compliance

GHGSat's satellites use an on-board spectrometer to acquire pixel information that swings as the sensor passes over an area. The mean spatial resolution expressed in FWHM of LSF is 2.2 pixels, and the mean effective footprint size is 67.0 m. A full table of results can be found below in Table 1. It should be noted that the Golden Gate Bridge image taken by sensor C7 contained a bridge shadow, making the background irregular. The non-shadow side was mirrored to keep the image in the analysis, this result is thus less reliable than the others.

We consider two aspects when grading GHGSat's SSR, their pixel resolution and the claimed SSR. The evaluated SSR is twice the pixel size, which is typically not a good result. Meanwhile, GHGSat specifies a larger SSR than grid size in their documentation which is close to the effective footprint size we have evaluated here. However, the specified size is proprietary, and most users are probably not aware of it. The ratio our estimated SSR to their pixel size is within the Basic grading range.

Table 1. SSR analysis for the 3 sensors evaluated, by direction. C7*: This result is more uncertain than the others because this image had a bridge shadow impacting the results. The shadow was removed by mirroring the opposite side across the bridge center line. **, this result was measured at an apparent FWHM of 75.0 m and reduced to 70.0 m after considering bridge width impacts from modelling.

Sensor	Direction	Pixel Size (m)	FWHM (pixel)	Effective footprint (m)
C2	Row	29.4	2.5	73.5
C5	Row	32.6	2.0	65.2
C5	Column	27.0	2.3	70.0**
C7*	Row	28.2	2.1	59.2
Mean	**Both**	**29.3**	**2.2**	**67.0**

4.2 Absolute Positional Accuracy

4.2.1 Method

Evaluation of GHGSat geolocation accuracy is a relative assessment, with Landsat 8 and 9 band 6 (1.57 µm - 1.65 µm) as the reference. Both sensors have 30 m pixel sizes, and GHGSat's wavelengths are within the range of Landsat 8/9's band 6.

Locations of interest for geometric evaluation are those with distinct geometric shapes for use in a feature matching algorithm. At this scale, this includes features in urban locations such as large cities, forest edges, and land cover changes (i.e. desert to grassland). Usually, images with many lakes would also be ideal, but in the case of GHGSat, they mask some water bodies using NaN ("Not a Number"), this is further discussed in Section 4.2.2. We would like to note that this is a best-case scenario evaluation performed over locations with easy to match features. Often science teams work in remote locations without distinct features for geolocation, and thus in these areas, users can expect lower geolocation accuracy than what is reported here.

The assessment algorithm starts by determining the area of overlap between reference and target images. This overlapped region is then split into subset image chips (690 m x 690 m). Each chip in the target image has a matching chip in the reference image based on the image geolocation metadata. The algorithm then imposes offsets on the target chip of the pair and calculates the Pearson Cross Correlation (PCC) coefficient (a measurement of how well two images match). The offsets that give the best PCC are taken to be the geolocation offset between the chip pair. Quality of chip co-registration is then calculated with a Measurement Uncertainty equation [De Luccia et al., 2016] used to filter out poor-quality chip matches [Semple et al., 2023].

Ten globally distributed locations were evaluated. Two of these are located at ~70°N in Alaska, USA. Results at these locations will be displayed separately, due to both their unique behavior and fewer chip matches (see section 4.2.2). The other locations include two USA locations, two in Russia, two in South Sudan, and one in Argentina.

GHGSat sometimes marks 'low quality' data as NaN in their surface reflectance product. However, this is not a consistent marking, some images contain their values despite being marked

'low quality' in the associated quality flag file. The quality flags are found in an associated flag file (*flg.tif) that is delivered with the standard product download. No explanations are given as to why pixels are marked as low quality.

We found that many water bodies in the far northern region of Alaska, USA (~70°N) are marked as NaN. Normally at this scale, edges of water bodies would be ideal for our geolocation assessment. However, our algorithm discards assessment chips containing the NaN designation because the NaN is a "hole" in the GHGSat imagery that cannot be matched with the reference images. This results in fewer, if any, chip matches in a GHGSat image over a region with a large quantity of 'low quality' flags. Thus, geometric assessment locations that are reliant on water bodies, such as the four Alaska North Slope locations in this evaluation, have less certain results due to the low number of expected chips used in the assessment. The offsets determined at the two Alaska North Slope evaluation locations were also visually confirmed because of fewer matches in this region.

4.2.2 Results Compliance

GHGSat claims a sub-pixel geolocation accuracy. Their pixel size is 30 m, and nothing more specific than "sub-pixel" is given.
We find that the GHGSat geolocation accuracy meets the vendor's claim for sites observed between the latitudes of 65°N and 34°S (Fig. 7) and does not meet the claim at latitudes at around ~70°N and above (Tables 2 and 3). Images acquired in the Alaska North Slope locations (~70°N) were found to vary in accuracy by 1-3 pixels (30-90 m). We note the known difficulty in geolocating images outside of 60°N - 60°S due to less availability of reference imagery.

Table 2. Global geolocation offset results for the 7 evaluation locations between 65°N - 34°S.

Site	*Latitude*	*X Mean (m)*	*Y Mean (m)*	*CE90 (m)*	*Images*
Russia3	65°N	5.0	14.8	23.7	6
Russia2	61°N	4.4	13.0	19.0	9
PA, USA	40°N	5.0	14.6	21.5	6
IL, USA	39°N	6.6	5.6	7.1	10
Iraq	33°N	7.5	-4.4	18.2	4
S. Sudan2	9°N	5.2	-7.0	12.6	8
S. Sudan1	8°N	6.6	7.6	14.3	6
Argentina	34°S	7.6	-5.0	10.7	21
Total	**65°N-34°S**	**6.2**	**5.9**	**15.3**	**70**

Table 3. Geolocation offset results for the 2 northern Alaska locations at 70°N.

	Latitude	*X Mean (m)*	*Y Mean (m)*	*CE90 (m)*	*Images*
AK1	70°N	10.6	55.1	55.3	7
AK2	70°N	26.8	-34.3	53.4	6
Total	**70°N**	**20.2**	**10.4**	**56.6**	**13**

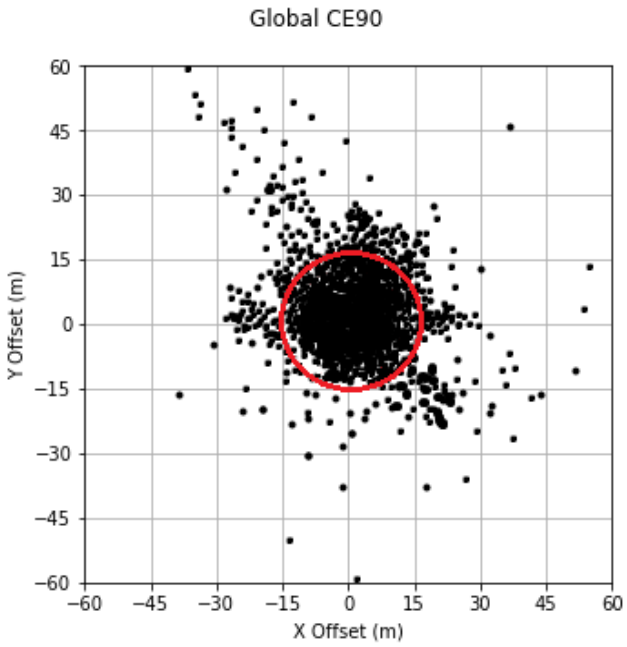

Figure 7. Plot of relative offsets for all locations except Alaska. The CE90 (red circle) is 15.3 m

Some GHGSat images were found to have warping at the edges, this was most prominent in the North Slope of Alaska imagery. Out of all images examined (80), 5 had a warping issue, one of which was outside of Alaska. The Alaska locations had a higher degree of warping, from 1-4 pixels. While the one location in Argentina had sub-pixel warping. Figure 8 shows an example of the worst warping found in this evaluation. Two GHGSat images are overlaid on top of each other by their geolocation information, one false colored in red, the other in blue. This coloring makes it easier to visually identify the offsets between the images, where the two images match, the pixels will be a grayscale, and where they do not, the pixels will be red or blue, depending upon the direction of the offset. Figure 8 demonstrates visually how the right and left edges of the images are shifted many pixels in opposite directions (Fig 8 b & d). The variation in the offset and offset direction across this image indicates that the two images are not simply shifted from each other, but one or both images are warped overall. Both images were removed from the overall evaluation.

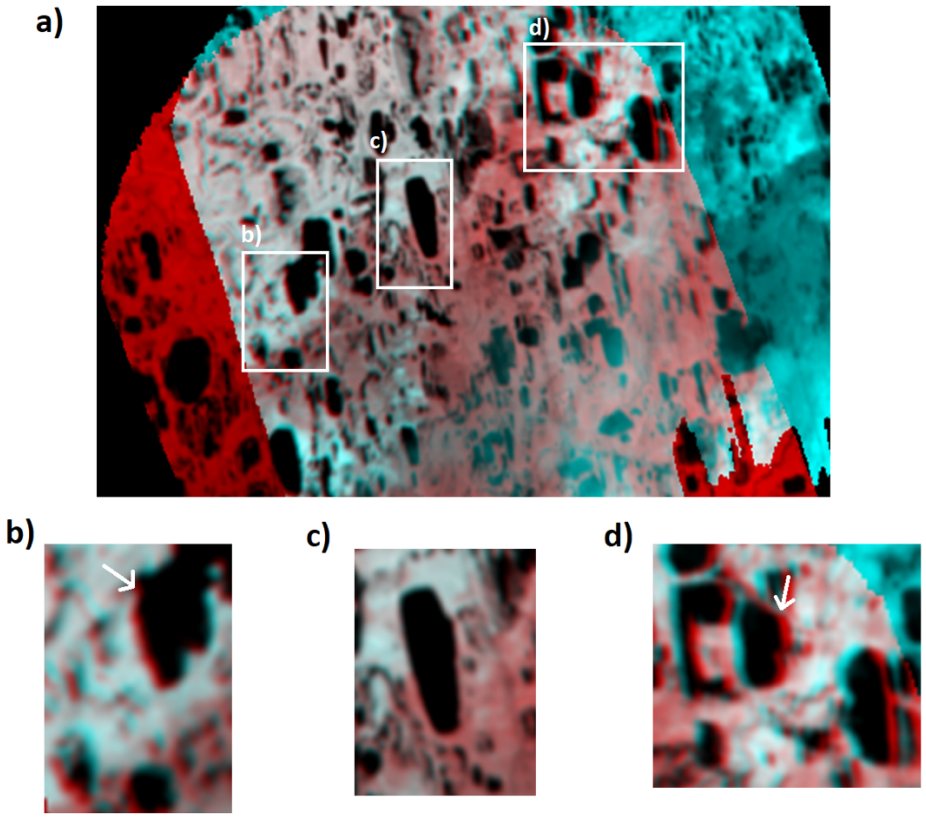

Figure 8. Warping in a GHGSat image over Alaska's north slope. Two GHGSat images were falsely colored red and blue and were overlain. Where the two images align, the image is grayscale. The large image shows the overall image, and the white boxes outline the regions magnified below. In region b) the red image is shifted ~70 m west (arrow points out red shift on the left side of the lake), whereas there is no shift between the images in region c). In region d), the red image is shifted ~120 m (4 pixels) east (arrow points out red shift on the right side of the lake). The offset changes in both magnitude and direction across the two images compared, indicating that one or both images are warped.

4.3 Temporal Stability

4.3.1 Method

Temporal stability is assessed with the image matching algorithm that is described above in section 4.2.1. Each location is assessed with the earliest GHGSat image in the set as the reference image. Our longest time series in the evaluation sample is at the Buenos Aires, Argentina location, with 21 images ranging from May 2021 to August 2022.

4.3.2 Results Compliance

GHGSat does not make claims on temporal stability beyond the specification that geolocation accuracy is less than 1 pixel. Other than the Alaska North Slope locations, most locations perform well enough for end-users interested in conducting timeseries analyses to process the data as delivered. Figure 9 shows time series analysis of offsets between the 21 images analyzed over

Buenos Aires, Argentina. Because of this, we give GHGSat's temporal stability a grade of Excellent.

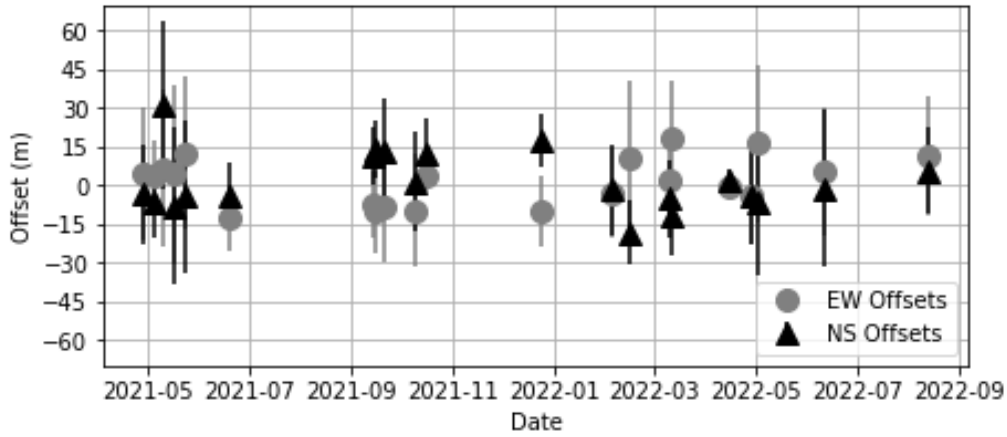

Figure 9. Mean offsets at Buenos Aires, Argentina for 21 images from over a year of data. East-West offsets are plotted in gray, while North-South offsets are in black. Standard deviations of each measurement are indicated by vertical bars. One image in this set of 21 has a 1 pixel (30 m) offset from the rest of the time series.

5 Atmospheric Column Product Overall Grade

The overall score for the GHGSat atmospheric column product is Good. In general, the different CSDA evaluation teams were able to quantify emissions from this product that were consistent with the GHGSat reported emissions product. There is a published paper that describing the sensor and measurements (Jervis et al., 2021) and a white paper that describes the metrics and validation of the products (McKeever and Jervis, 2022). GHGSat has also produced an ATBD document, but this document, among others provided to CSDA by GHGSat, are marked as proprietary. Weaknesses reducing the score were related to traceability of the data back to the original satellite measurements and a lack of validation that can directly test the quantified column enhancements and their uncertainties.